Ligand-Mediated Mechanical Enhancement in Protein Complexes at Nano- and Macro-Scale

Samuel Kim[a], Marcus V. J. Cathey[a], Brandon C. Bounds[a], Zackary Scholl[b], Piotr E. Marszalek[b], Minkyu Kim[a,c,d]*

[a]Department of Biomedical Engineering, University of Arizona, Tucson, AZ, 85721, USA

[b]Department of Mechanical Engineering and Materials Science, Duke University, Durham, NC, 27708, USA

[c]Department of Materials Science and Engineering, University of Arizona, Tucson, AZ, 85721, USA

[d]BIO5 Institute, University of Arizona, Tucson, AZ, 85719, USA

Keywords: protein complex, ligand, artificial protein design, molecular self-assembly, nanomechanics, hydrogel, bulk mechanical properties

Abstract

Protein self-assembly plays a vital role in a myriad of biological functions and the construction of biomaterials. Although the physical association underlying these assemblies offer high specificity, the advantage often compromises the overall durability of protein complexes. To address this challenge, we propose a novel strategy that reinforces the molecular self-assembly of protein complexes, mediated by their ligand. Known for their robust non-covalent interactions with biotin, streptavidin (SAv) tetramers are examined to understand how the ligand influences the mechanical strength of protein complexes at the nanoscale and macroscale, employing atomic force microscopy-based single-molecule force spectroscopy, rheology, and bioerosion analysis. Our study reveals that biotin binding enhances the mechanical strength of individual SAv tetramers at the nanoscale. This enhancement translates into improved shear elasticity and reduced bioerosion rates when SAv tetramers are utilized as crosslinking junctions within hydrogel. This approach, which enhances the mechanical strength of protein-based materials without compromising specificity, is expected to open new avenues for advanced biotechnological applications, including self-assembled, robust biomimetic scaffolds, and soft robotics.

Introduction

Interactions of self-oligomerizing biopolymers, such as proteins, play a crucial role in various biological processes, such as intercellular communication and the self-assembly of supramolecular structures (e.g., actin filaments, hemoglobin, virus capsid).[1-4] Moreover, utilizing self-associating protein complexes as physical cross-linkers is advantageous for constructing intricate, biomimetic materials that require high specificity for biotechnological applications.[5-8] However, due to their relatively fast erosion stemming from weak strength of physical interactions (e.g., hydrogen bonding, hydrophobic interactions), such cross-linkers can lead to a short lifetime for self-assembled structures when compared to chemically-crosslinked structures.[9] To enhance the stability of physically cross-linked materials, while maintaining high specificity, there is a need to develop a strategy that can modulate the mechanical strength of protein complexes.

We propose that the strength of self-association within protein complexes can be controlled by ligand binding onto the complex. This hypothesis is based on observations that are indicative of multiple biophysical effects of ligand binding on individual protein domains[10] or subunits of a protein complex[11], such as converting mechanical unfolding features, altering folding kinetics, and enhancing the mechanical stability of the folded structure.[10-15] Nevertheless, the implication of ligand binding on the mechanical strength of protein complexes across multiple length-scales remains unexplored. By identifying a model protein complex capable of ligand binding, we can investigate how ligand binding regulates the mechanical behaviors of self-assembled protein complexes at the nanoscale and even larger scales (**Figure 1**).

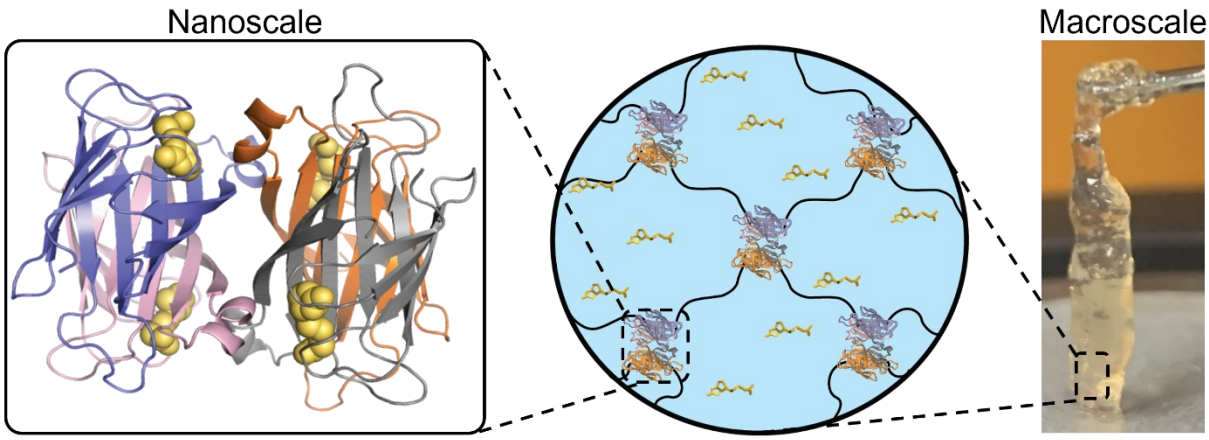

Figure 1. Probing the influence of ligand binding on mechanical behaviors of protein complexes at the nanoscale and macroscale. Atomic force microscopy-based single-molecule studies can elucidate the nanomechanical impact of ligand binding (yellow spheres at the left panel) on protein complexes (PDB ID: 1SWE). The obtained insight can be utilized to design polymer networks and hydrogels crosslinked by these protein complexes. The correlation between the nanoscale and macroscale mechanical behaviors of protein complexes under different ligand conditions can be established through bulk material testing methods, such as rheology and bioerosion.

In this study, we chose streptavidin (SAv) tetramer as the model protein complex, known to exhibit one of the strongest non-covalent interactions with its ligand, biotin. This interaction occurs in a 4:4 stoichiometric ratio with a dissociation constant (K_d) of 10^{-14} - 10^{-16} M.[16-23] Based on extensive studies of the crystal structures, the SAv tetramer is self-assembled from four identical SAv monomers. These monomers bind tightly to form dimers, which then self-associate with somewhat less tightness than the monomer-monomer interaction, ultimately leading to the formation of a tetramer (**Figure 2**A).[16, 17, 24-26] Biochemical properties revealed the enhanced thermal stability of SAv tetramers upon biotin binding.[16-18, 24, 25, 27] In a previous study using atomic

force microscopy (AFM)-based single-molecule force spectroscopy (SMFS) on SAv tetramers with 10 μM biotin and a pulling speed of 500 nm/s, we observed that the dimer-dimer interface ruptures at around 100 pN, while the monomer-monomer interfaces rupture at approximately 400 pN.[28] However, SAv tetramers in the absence of biotin or with different biotin concentrations have yet to be examined at the single-molecule level. Moreover, the impact of biotin binding on the mechanical behavior of macroscale materials composed of such protein complexes is yet to be determined.

Utilizing AFM-based SMFS, rheology, and bioerosion analysis, we were able to comprehensively examine the biotin-mediated mechanical behaviors of the SAv tetramer. Each technique offers a unique perspective: AFM-based SMFS allows for the investigation of biotin-mediated nanomechanics of individual SAv tetramers and rheological characterization and bioerosion testing evaluate the mechanical behaviors of SAv-crosslinked polymer networks and hydrogels at the macroscale. This study presents a novel, straightforward strategy to modulate the mechanical behaviors of not just protein complexes like SAv tetramers, but also potentially more elaborate structures that incorporate protein complexes and have ligand binding capabilities. Furthermore, this research provides insight into the fabrication of customizable and tunable supramolecular materials for diverse biotechnological systems, ranging from drug delivery vesicles[29] to biomimetic scaffolds[8] and soft robotics.[30]

Results and Discussion

Reinforced the weak dimer-dimer interface of SAv tetramer upon biotin binding. To evaluate the influence of biotin on the mechanical integrity of individual SAv tetramers, we employed AFM to measure the rupture strength of SAv tetramers under different biotin conditions.

For this purpose, we genetically fused a protein-based force probe[31] composed of alternating tandem domains of I27 and staphylococcal nuclease (SNase) to the N-terminus of a SAv monomer (Figure 2B). This force probe, consisting of mechanically strong (i.e., I27) and mechanically weak (i.e., SNase) domains, serves as a handle for AFM stretching measurements across three different directions (Figure 2C). It acts as an internal force standard and provides an unmistakable fingerprint of true single molecule recordings. AFM studies revealed that, at a pulling speed of 500 nm/s, SNase and I27 domains unfold at approximately 30 pN with ~ 45 nm of contour length increments (ΔLc)[31] and 200 pN with ~ 28 nm of ΔLc,[32] respectively. The unique unfolding patterns of SNase and I27 served as an unambiguous detection of rupture forces (i.e., $\geq$ 30 pN) of individual ligand-receptor pairs and protein-protein complexes.[31] Using these force probes, a molecular bridge can be easily formed through non-specific adsorption between an AFM tip and a substrate that can be stretched until the protein complex of interest ruptures and breaks apart (Figure 2D). We opted for non-specific adsorption instead of specific attachment of molecules to the substrate[33] due to the inherent structural complexity of SAv tetramers. Specifically, the homotetrameric nature of SAv, featuring multiple potential binding sites, complicates the use of specific interactions and could lead to less frequent measurements in our single-molecule force spectroscopy. This understanding informed our strategy to use non-specific interactions with the force probe, ensuring clear and reliable data collection. Consequently, when three SNase domains flank the protein complex, such as SAv tetramer, any force-extension recording containing four or more SNase domains indicates that the probes have been picked up on either side of the protein complex. The final force of such a recording can result from either the rupture strength of the protein complex or the force of detachment of the protein force probe from the substrate or the AFM cantilever. To distinguish the rupturing forces of the protein complex from the detachment events, we compared

the distribution of final force peaks of force probes with and without the protein complex (Figures 2E-F and Figure S1).[31]

Figure 2D presents a representative example of AFM force-extension curves of the single [(SNase-I27)$_3$-SAv monomer]$_4$ complex, which exhibited four or more SNase unfolding force peaks that fulfilled our criterion and were subsequently selected for further analysis. In the AFM force-extension curve, six unfolding force peaks of SNase domains were observed, indicating that the final force peak (dashed circle) represent either the rupture force of the SAv tetramer or the detachment force of I27-SNase handles from the substrate or the cantilever. To determine the rupture strength of the SAv tetramer, the final force results of SAv tetramers with and without biotin were analyzed using kernel density estimation (KDE) and histogram methods, and then compared with detachment force results of I27-SNase handles alone (Figures 2E-F and Figure S1). These probability densities showed that the most frequent rupture force of SAv tetramers without biotin occurs at around 50 pN (Figure 2E). Comparing these final force events with detachment events at 50 pN allows us to identify that more than 50% of final forces at 50 pN represent rupture events of SAv tetramers in the absence of biotin. In the presence of 1 mM biotin, biotin did not significantly affect detachment forces when compared to the result without biotin (Figure S2). However, the center of the most frequent final force was shifted from 50 pN to 150 pN and had a greater proportion of events than the distribution of detachment events (Figure 2F). This indicates that the interfaces within SAv tetramers strengthened when 1 mM biotin was present.

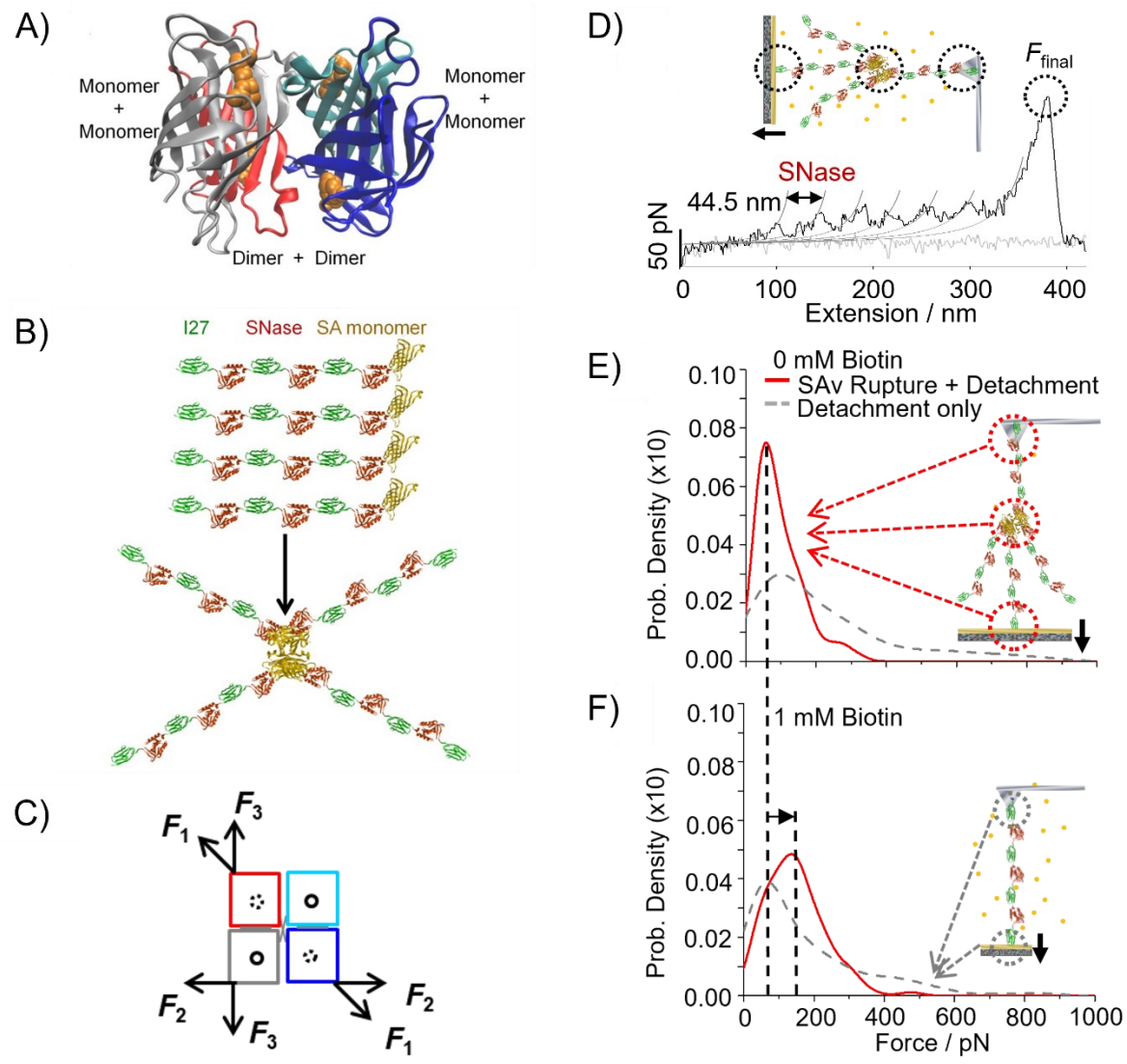

Figure 2. Biotin binding effect on the intermolecular strengths within SAv tetramer at a single-molecule level using nanoscale protein-based force probes fused SAv tetramer. (A) Crystal structure of biotin (shown as van der Waals sphere) and SAv tetramer (PDB ID: 1SWE); (B) A schematic of the $[(I27\text{-}SNase)_3\text{-}SAv\ monomer]_4$ complex self-assembled through four SAv monomers; (C) Three AFM pulling geometries (F_1, F_2, and F_3) can be applicable when AFM stretches the SAv tetramer through the $(I27\text{-}SNase)_3$ handles due to the connection of the handles to the N-terminus of each SAv monomer. Circles represent biotin binding sites (solid empty circle:

front, dashed empty circle: back).; (D) Representative AFM force-extension curve of [(I27-SNase)$_3$-SAv monomer]$_4$. Multiple gray lines are worm-like chain (WLC) model that fits to the curve with 44.5 nm of contour length increments (ΔLc) and 0.8 nm of persistent length (p) which correspond to the unfolding of individual SNase domains. The dashed circle on the curve represents either rupture events of a single SAv tetramer or detachment events of protein handles from the AFM cantilever or the substrate, depicted by the three dashed circles in the inset schematic.; (E) Probability densities of rupture forces, F_{final}, obtained from [(I27-SNase)$_3$-SAv monomer]$_4$ (solid curve; N = 91) and of detachment forces, $F_{\text{detachment}}$, from I27-(SNase-I27)$_3$ handles alone (dashed curve; N = 160) without biotin; (F) Probability densities for F_{final} of [(I27-SNase)$_3$-SAv monomer]$_4$ (solid curve; N = 102) and $F_{\text{detachment}}$ of I27-(SNase-I27)$_3$ (dashed curve; N = 307) with 1 mM biotin. See Figure S1 for histogram results, Figure S2A for the representative force-extension curve of I27-(SNase-I27)$_3$ force probe, and Figure S2B and S2C for the whole detachment force range in the absence and presence of 1 mM biotin in the buffer. Schematics from Figure 2B and 2D-F were reprinted and adapted with permission from the referenced article.[28]

Considering the distinction between the rupture forces of the SAv tetramer and the detachment forces from the cantilever or the substrate (Figure S1), as well as previous work[28], we reason that the most frequent final forces (Figures 2E and 2F) mainly reflect rupture events of the SAv dimer-dimer interface. The SAv dimer-dimer interface has less interfacial surface area and fewer hydrogen bonds than the monomer-monomer interfaces based on the crystal structures.[16, 17, 26, 28] Additionally, the distributions shown in Figures 2E and 2F have long tails that extend up to 500 pN, whereas the distribution of detachment has events extending to 1000 pN. These results

suggest that 50 pN in Figure 2E and 150 pN in Figure 2F represent rupture events of the weak SAv dimer-dimer interface, while the long tails in both distributions could be related to rupture events of strong monomer-monomer interfaces. Consistent with these results, our observations show the most frequent rupture force of the dimer-dimer interface to be at 100 pN when 10 μM biotin is present.[28] Therefore, we can confirm that biotin binding can enhance the mechanical strength of the dimer-dimer interface in individual SAv tetramers.

This finding can be due to the improved association of the weak dimer-dimer interface within the SAv tetramer, induced by the presence of biotin. The enhancement of thermal stability of SAv tetramers has been suggested to be due to the tighter association of the dimer-dimer interface, attributed to the diagonal contact between tryptophan (W)120 from SAv monomer (cyan in Figure 2A) and biotin in across SAv monomer (gray in Figure 2A) within the SAv tetramer.[17, 25, 34] Similarly, our results indicate that the mechanical stability of the SAv tetramer was reinforced upon biotin binding (Figures 2E and 2F), potentially caused by the tighter association of the dimer-dimer interface.

Mechanical enhancement of SAv-crosslinked hydrogels upon biotin binding. Although the biotin binding to SAv tetramers enhanced their weak dimer-dimer interfacial strength at the single-molecule level, it remains unclear if, and how this effect can be observed at the macroscale. To elucidate the macroscopic implications of ligand binding to its protein receptors, we designed and synthesized artificial proteins that can be self-assembled and fabricated into protein hydrogels. These engineered hydrogels consist of a polymer network with interconnected SAv tetramers serving as network junctions. This approach enables effective mechanical characterization of the hydrogels, providing insights into the influence of biotin-mediated effects on SAv-crosslinked bulk materials.

A previous study demonstrated that an additional crosslinking mechanism with high specificity and strength is required to promote the formation of a protein-based polymer network with self-assembled junctions of SAv tetramers.[35] For this purpose, we utilized the "SpyTag-SpyCatcher" split protein system[36, 37] as the complementary crosslinking mechanism to the SAv tetramer cross-linker (**Figure 3**). The key feature of this profound crosslinking mechanism involves the formation of an isopeptide bond between the Lys31 of SpyCatcher (SC) and Asp117 of SpyTag (ST) immediately after the self-association of these two biomolecules.[36, 37] Specifically, we biosynthesized two artificial protein constructs to prepare SAv-crosslinked polymer networks. The first construct is a self-associated SAv tetramer with four ST, each genetically fused to the C-terminus of every SAv monomer, referred to as (SAv monomer-ST)$_4$ (Figure 3A). The second construct, denoted as SC-C_{24}-SC, includes an intrinsically disordered, flexible C_{24} protein composed of 24 repeats of the AGAGAGPEG amino acid sequences[9, 38], with SC on each terminus (Figure 3B). Separately prepared protein solutions, containing (SAv monomer-ST)$_4$ or SC-C_{24}-SC, were mixed in 1:1 molar ratio between ST and SC. The formation of covalent bonds after specific binding between SC and ST enabled the protein network under aqueous conditions and generated a hydrogel (Figure 3C).

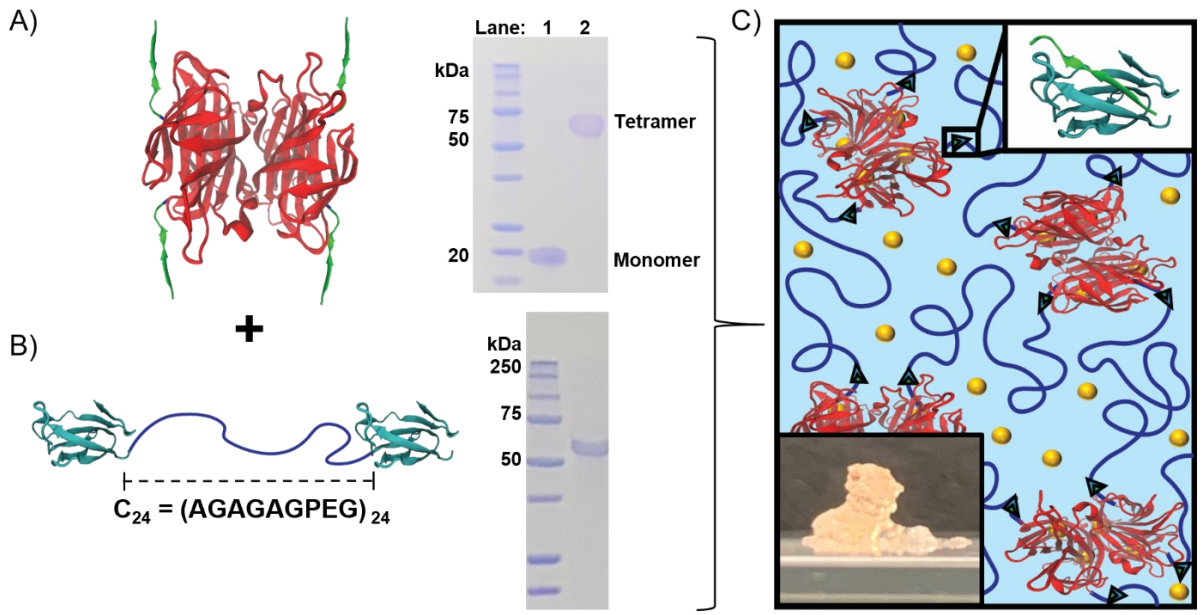

Figure 3. Schematics and SDS-PAGE analysis of purified artificial protein constructs used for fabricating SAv-based hydrogels. (A) After genetically fusing ST to the C-terminus of SAv monomer, SAv tetramer with four SpyTag (ST) were biosynthesized and self-associated (SAv monomer-ST)$_4$. The SDS-PAGE analysis illustrates the purity of lyophilized protein samples and the molecular self-assembly capability of SAv. Lane 1 shows SAv tetramers denatured to monomers by boiling samples at 100 °C. Lane 2 depicts the native conditions leading to SAv tetramer formation, demonstrating the successful molecular self-assembly of SAv post biosynthesis.; (B) SpyCatcher (SC) was genetically fused at each terminus of a flexible, intrinsically disordered protein, known as C_{24}, resulting in SC-C_{24}-SC. The SDS-PAGE analysis shows high sample purity, but slightly greater molecular weight (M.W.) than the theoretical M.W. (41.60 kDa). LC/MS analysis reveals that the sample M.W. matches the theoretical M.W. (Table S1). The greater M.W. observed on SDS-PAGE is attributed to the presence of C_{24} protein, as established in previous studies.[38]; (C) By combining separately prepared protein solutions at a final

1:1 molar ratio between ST and SC, hydrogels composed of a polymer network were constructed and characterized with different concentrations of biotin (represented by gold dots).

By visual inspection, we immediately identified that the addition of biotin caused the hydrogels to be compact (**Figure 4A**). To quantify this finding, we evaluated the mechanical strength of SAv-based hydrogels at different concentrations of biotin using small amplitude oscillatory shear rheology. We compared the shear elastic modulus (G′) through strain and frequency sweep measurements (Figure 4B; Figures S3 and S4). The results indicate that biotin binding to SAv tetramers significantly improves the experimental G′ of the hydrogel (Figure 4C; Table S2). When examining the experimental G′ at 0.5 mM and 1 mM biotin concentrations, we observed values of 339.81 ± 18.31 Pa and 856.83 ± 58.20 Pa, respectively. These data reveal a 32% increase in the experimental G′ at 0.5 mM and a dramatic 232% increase at 1 mM, relative to the baseline value of 257.85 ± 65.94 Pa at 0 mM biotin. Based on substantial improvements in G′ at 1 mM of biotin, we decided to further increase the biotin concentration to 10 mM. The hydrogel, containing approximately 3.6 mM of SAv tetramer, exhibited a slight increase in the experimental G′ to 954.79 ± 80.72 Pa, compared to the 1 mM biotin concentration. Although the difference between the average G′ obtained at 1 mM and 10 mM of biotin was not statistically significant, it was evident that the addition of biotin substantially influenced the shear elasticity of the SAv-based hydrogels.

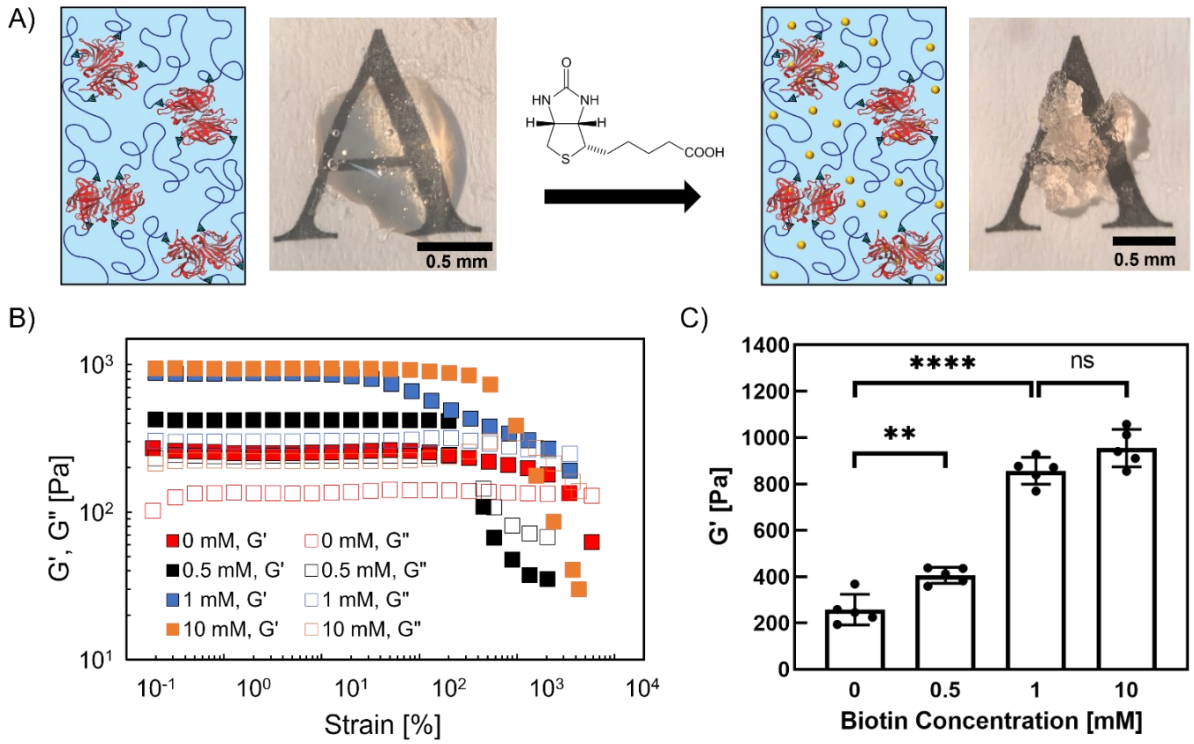

Figure 4. Visual inspection and rheological characterization of SAv-based hydrogels with different biotin concentrations. (A) Microscope images of SAv-based hydrogel with schematics of polymer networks in the absence and presence of biotin; (B) Representative strain sweep data for SAv-based hydrogel samples with different biotin concentrations; (C) Experimental G′ with different biotin concentrations (all data are available in Figure S3; $N = 5$; **p < 0.01; ****p < 0.0001; ns = not significant; see Table S2).

However, to confirm that these results were exclusively due to the biotin binding to SAv tetramers used as junctions in the hydrogel, additional control experiments were performed. In these experiments, we fabricated and characterized hydrogels wherein the SAv junctions were replaced with pentameric protein complexes composed of self-assembling coiled-coil cross-linkers (Figure S5A).[38] As expected, there were no significant changes of experimental G′ regardless of

the biotin concentration (Figure S5B). Furthermore, we designed another control experiment by replacing the flexible C_{24} midblock (Figure 3B) with a more rigid structure using a synthetic version of ankyrin, a spring-like protein found in the cytoskeleton of red blood cells (SC-NI_6C-SC; Figure S6).[38, 39] Despite changing the midblock with different strand rigidity, there was still a significant increase in experimental G′ across different biotin concentrations (Figures S7 and S8; Table S2). As a result, these additional controls validate the experimental results (Figure 4) and support the notion that the biotin binding on SAv junctions in the polymer network can enhance the overall mechanical properties of these hydrogels.

Given the disparity in multi-length scale and insight between AFM-based SMFS and rheology, it is difficult to directly correlate the mechanical reinforcement of individual SAv tetramers at the nanoscale with the observed improvement in the shear elasticity of SAv-based hydrogels. It has been demonstrated that controlling the dissociation of cross-linkers can affect the gel relaxation.[40-43] However, this control did not show a discernible effect on shear elasticity, as assessed from the plateau G′ of the polymer network, distinct from our results (Figure 4C).

Instead, previous research demonstrated that biotin binding to the SAv tetramer induces a tightened association of the dimer-dimer interface within the SAv tetramer.[17] Based on this information, we propose that the collective change in multiple SAv structures significantly contributes to the mechanical enhancement of the overall hydrogel comprised of SAv tetramers as network junctions. With approximately 49% of the polymer network consisting of SAv tetramers, it is plausible that nearly half of the polymer network may experience structural changes, upon biotin binding. These changes could increase residual stress in the C_{24} proteins, which are located between the SAv junctions (Figures 3C). This conjecture, coupled with the visual inspection in Figure 4A, suggests an indirect correlation between nanoscale and macroscale findings.

To directly compare nanoscale and macroscale results, one can conduct tensile tests on bulk SAv-based materials with varying biotin concentrations. This method is effective because of its similarity to the AFM-based SMFS technique used for measuring protein nanomechanics. However, this SAv-based polymer network design, despite demonstrating mechanical enhancement of SAv tetramers in the presence of biotin, exhibited limitations in overall strength. It is not sufficiently strong enough for tensile testing, primarily due to the presence of network defects.[44] When examining the experimental G′ of the hydrogel with 10 mM of biotin, it was only 15.97 ± 1.35% of the theoretical G′, calculated by the Affine network model[45] (Table S3). The major cause of network defects can be attributed to the inhomogeneous crosslinking density, a result of spontaneous chemical crosslinking after the specific molecular self-assembly between the ST and SC.[35] The rapid formation of the isopeptide bond does not provide enough time for the SAv tetramers to adequately diffuse throughout the polymer network. Given these challenges and the absence of an effective crosslinking mechanism offering temporal control without interfering with the molecular self-assembly of the SAv tetramer, we have chosen to investigate ligand-mediated mechanical behaviors of protein complexes at the macroscale using the ST-SC system. For this reason, it is evident that further optimization to our SAv-crosslinked polymer network design is needed, or a different type of macroscale experiments is required to directly correlate nanoscale results to the macroscale.

Improvements in bioerosion rates in SAv-based hydrogels upon biotin binding. To further explore the impact of biotin-mediated mechanical reinforcements of SAv tetramers in bulk materials, we took an alternative approach and conducted bioerosion experiments. Bioerosion, resulting in the loss of mechanical strength and structure due to the breakdown of cross-linked sites in a polymer network[46], was considered a suitable method to examine whether the biotin

binding can reinforce and strengthen SAv-based hydrogels at the macroscale. In this investigation, we evaluated the erosion rate of SAv-based hydrogels with and without biotin under erosion-promoting conditions at 37 °C (**Figure 5**A). Based on the rheological characterization (Figure 4C) and SDS-PAGE analysis on the thermal stability of SAv tetramers in various biotin concentrations (Figure S9), we chose a biotin concentration of 10 mM for the bioerosion testing of SAv-based hydrogels. Our analysis revealed distinct erosion rates during two specific timeframes: 0-4 hours and 4-48 hours (Figure 5B). Regardless of the presence of biotin, all hydrogels exhibited a significant increase in the absolute erosion rate within the initial 0-4 hours, ranging approximately 280-300%, compared to the subsequent 4-48 hours. This rapid erosion rate during the initial stages can be attributed to the presence of non-crosslinked proteins within the polymer network, increasing the likelihood of detaching from the hydrogel in the aqueous buffer (Figure 5A). To ensure a more accurate assessment of the erosion process of SAv junctions, our analysis focused on the erosion rate between 4 and 48 hours where the hydrogel stability has become more established.

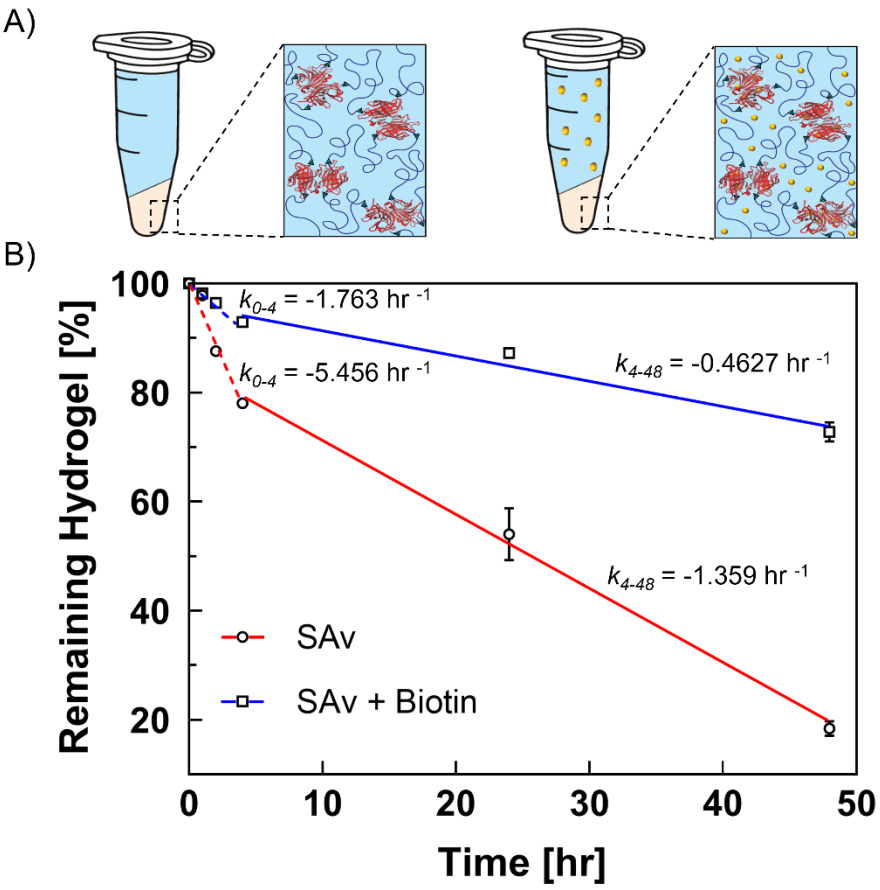

Figure 5. Bioerosion experiment of SAv-based hydrogel in the presence and absence of 10 mM biotin. (A) Schematic of bioerosion tests and polymer networks of hydrogels, denoted as beige color. All bioerosion experiments were performed with a 1:9 volume ratio of the hydrogel:solvent, with or without biotin (gold dots) at 37 °C.; (B) Bioerosion graph depicts erosion rates over time (slope *k*; eroded hydrogel % / hour). Simple linear regression analyses were conducted for the following time intervals: 0-4 hours (dotted lines) and 4-48 hours (solid lines). The sample size of each time point was in triplicate ($N = 3$).

Within the time frame of 4-48 hours, we observed 66% decrease in the erosion rate of SAv-based hydrogels in the presence of biotin when compared to the hydrogels without biotin in the

aqueous buffer at 37 °C (Figure 5B). Using these erosion rates, we calculated the half-life of the hydrogels with biotin to be approximately 100 hours, while the half-life of the hydrogels without biotin was only about 25 hours. This substantial 300% increase in the half-life indicates that the biotin binding mediates the mechanical enhancement of the individual SAv tetramers, reinforcing the junctions in the polymer network and effectively delaying hydrogel erosion over time. While the ST and SC system used in the hydrogels may contribute to bioerosion[47], the distinct difference observed with biotin suggests the ligand's predominant role in reinforcing the SAv-based hydrogels. Therefore, these findings establish a correlation between the nanoscale mechanical reinforcement observed in AFM-based SMFS studies and the improved erosion resistance at the macroscale, emphasizing the critical role of ligand-mediated mechanical reinforcement of protein complexes across multiple length-scales.

Supplementary bioerosion tests were also conducted to evaluate SAv-based hydrogels to comprehend the behavior of SAv tetramers as network junctions under different conditions. For example, the impact of incubation temperatures on SAv-based hydrogels were assessed (Figure S10A). The half-life of the hydrogel increased from 100 hours to approximately 330 hours when the temperature decreased from 37 °C to 25 °C, respectively. Another comparative study was also performed contrasting hydrogels with self-assembled pentameric coiled-coil cross-linkers and hydrogels with SAv cross-linkers (Figure S10B). As predicted, hydrogels without SAv tetramers demonstrated a significant reduction in the half-life (~2.5 hours) when compared to the hydrogels with SAv cross-linkers (~330 hours). These additional experiments provide perspective into the strength of SAv tetramer as a physical cross-linker, when compared to the other well-known, physical cross-linkers.[9, 38, 48]

Conclusion

Our investigation elucidated the impact of ligand binding on protein complexes using a well-known model, SAv tetramer and biotin, across multiple length-scales. At the nanoscale, using AFM-based SMFS, we validated that biotin binding mechanically reinforced the weak dimer-dimer interface of individual SAv tetramers. Building on this result, we genetically incorporated SAv tetramers into artificial protein polymer network designs, fabricated SAv-based hydrogels and evaluated the mechanical impact of biotin binding at the macroscale. Not only did these hydrogels demonstrated significant enhancements in mechanical strength in polymer networks, caused by the biotin binding effects to the SAv network junctions, but they also exhibited a substantial decrease in erosion rates, indicating improvements in the lifespan of SAv-based hydrogels in aqueous buffer. This discovery, demonstrating that biotin binding effects at the nanoscale can influence the overall polymer network composed of SAv junctions, presents a straightforward approach for mechanically tuning self-assembled protein complexes, along with potentially developing more sophisticated architectures with enhanced stability.

The ability to modulate the mechanical strength of self-assembled protein complexes unlocks opportunities for fabricating customizable supramolecular systems. This control empowers the creation of adaptable and intricate materials, including elasticity-controllable tissue scaffolds, enabling precise mimicry of target tissue elasticity for stem cell specialization.[49] In soft robotics, overall stiffness of soft materials, composed of the protein complexes, can be readily modulated by varying the ligand concentration in an aqueous environment, leading to mechanically adaptive shape changes.[30] Therefore, probing the interaction of protein complexes and their ligands can emerge as a novel and transformative approach for developing mechanically tunable supramolecular platforms in a simple fashion.

METHODS

Sample Preparation for AFM-based Single-molecule Force Microscopy. Amino acid sequences for [(I27-SNase)$_3$-SAv monomer]$_4$ and I27-(SNase-I27)$_3$ constructs were recorded in Table S4. Both constructs were prepared by the method as described previously.[28] 1 mg/mL of all proteins were diluted to 10-100 μg/mL by the buffer containing 100 mM Tris-HCl (pH 7.6), 150 mM NaCl, 1mM EDTA, and 1mM Tcep with or without 1 mM biotin (product # B4501, Sigma-Aldrich, St. Louis, MO, USA). Fresh Au cover slips were prepared right before the protein incubation on those substrates in order to provide similar surface conditions. Au coated glass cover slips were sonicated in acetone and then ethanol for 3 minutes each. [(I27-SNase)$_3$-SAv monomer]$_4$ and I27-(SNase-I27)$_3$ proteins were incubated on fresh Au substrates. 50 μL of protein solutions with 5 ~ 20 μg/mL concentration were used for all samples. After 40 minutes of incubation at room temperature, all proteins were gently washed by the buffer and ready for AFM pulling experiments.

AFM-based Single-molecule Force Spectroscopy Measurements. Measurements of rupture forces or detachment forces of protein complexes were performed by our custom-built AFM instruments[50, 51] with MSNL AFM cantilevers (Bruker AFM Probes, Santa Barbara, CA, USA). 10 ~ 18 pN/nm of AFM cantilever spring constants were obtained in solution at room temperature by using the energy equipartition theorem.[52] The cantilever produced ~10 pN of RMS force noise in the 1-500 Hz bandwidth. To avoid obtaining final force results from the same molecule, AFM tip only pulled molecules once at each location. An AFM automation automatically adjusted Z-axis to perform force extension experiments while the X-Y locations were raster scanned across the

surface. Usable force-extension curves were recorded automatically if they fulfilled heuristics present in "good" recordings.[53]

Protein Expression for SAv-based Hydrogel Characterization. Protocol was based on the referenced articles.[35, 38] Amino acid sequences for (SAv monomer-ST)$_4$, SC-C$_{24}$-SC, SC-NI$_6$C-SC, and P-C$_{24}$-P constructs were recorded in Table S4. Gene sequences were inserted into the pET24a expression plasmids using BamHI, Xhol restriction enzymes (GenScript, USA). The resulting plasmids were then transformed into BL21(DE3) *Escherichia coli* (New England Biolabs, USA) and grown on kanamycin-resistant agar plates for 12 hours. Single colonies were used to inoculate 5 mL of TB medium with 50 μg/L kanamycin, which were then grown in a shaking incubator at 37 °C and 220 RPM overnight. Then, 10 mL of the overnight culture was added to 2.8 L protein expression flask containing 900 mL TB media and 100 mL of potassium phosphate buffer with 1 mL of 50 mg/L kanamycin. These 1 L cultures were incubated at 37 °C and 250 RPM until optical density at a wavelength of 600 nm (OD_{600}) was between 0.5 to 0.7, which was measured using a Cary 60 UV-vis spectrophotometer (Agilent Technologies, USA). Once the OD_{600} reached the absorbance range, 500 μL of 1 M isopropyl β-D-1-thiogalactopyranoside (IPTG) was added to every 1 L culture, which induces protein expression, and the cultures were incubated overnight at 24 °C and 220 RPM. Using centrifugation, cells were harvested in 4 °C at 7,000 x g for 10 minutes. Cell pellets from each 1 L expression were first suspended in 200 mL of 50 mM sodium phosphate and 300 mM sodium chloride (pH 7.6), and then frozen at -80 °C for at least 1 hour. For (SAv monomer-ST)$_4$ expression, cell pellets must be resuspended in the same buffer with 8 M Urea to prevent any formation of inclusion bodies.[28, 54]

Protein Purification for SAv-based Hydrogel Characterization. Purification method was based on the referenced articles. [35, 38] Frozen, resuspended cell pellets were thawed and transferred into

500 mL wide-mouth bottles. The resuspended samples were sonicated three times for ten minutes each using a Branson Sonifier 250 (Branson Ultrasonics, Danbury, CT, USA) at an output power of 5 and a duty cycle of 50%. Once the sample viscosity resembles the viscosity of water, the solution was poured into 500 mL centrifuge bottles and centrifuged for at 20,000 x g for 40 minutes at 10 °C. To further remove any more insoluble cell debris, the supernatant was aliquoted into 50 mL conical tubes and then centrifuged at 12,500 x g for 20-30 minutes at 10 °C. Then, the supernatant was stored at 4 °C. Due to the six Histidine amino acid residues on one of the termini, the desired proteins were purified and extracted via affinity column chromatography using Cobalt-Resin beads (Fisher Sci, Catalog: PI89965, USA). Column elutions were dialyzed in 4.5 L of 20 mM Tris buffer (pH 8.0), with a total of seven buffer changes occurring every three hours to remove any salts, impurities, and urea. Following the Tris dialysis, fast protein liquid chromatography was performed in 20 mM Tris buffer (pH 8.0) with an anion exchange column. Selected elutions were collected and dialyzed in 4.5 L deionized water following the same protocol as the Tris dialysis step to remove any impurities. After the entire purification procedure, all purified proteins were lyophilized and stored at -20 °C. Sample purity was evaluated using SDS-PAGE analysis after each purification step and using LC/MS after biosynthesis (see Table S1).

SAv-based Hydrogel Fabrication. All lyophilized protein constructs were dissolved in 20 mM Tris at 4 °C overnight. For the stock (SAv monomer-ST)$_4$ solution, biotin was added and dissolved to fulfill the desired final biotin concentration. Stock concentration of (SAv monomer-ST)$_4$ and SC-C_{24}-SC, or SC-NI_6C-SC, were mixed where the final concentration has a 1:1 molar ratio between ST and SC. Signs of gelation occurred within 5 minutes. To make sure all the possible self-assembly between ST and SC is completed, hydrogel samples were further incubated in 4 °C for 1 hour right before characterization.

Rheology. Mechanical properties of each hydrogel were characterized by small amplitude oscillatory shear rheology using the Discovery Hybrid Rheometer 2 (TA Instruments, New Castle, DE, USA) with a sandblasted 1°, 20 mm cone-plate geometry. Protocols were adopted from referenced articles.[35, 38] Before each experiment, inertia and friction of the geometry and rotational mapping calibrations were performed. All experiments were maintained at 25 °C using a Peltier temperature-controlled stage. To prevent evaporation, mineral oil was spread around the stage, and a solvent trap with a DI H_2O seal was placed over the geometry. Strain sweeps were conducted from 0.1-1000% shear strain at a constant angular frequency of 10 rad/s. G′ and G″ were calculated by averaging the values within the linear viscoelastic region (0.1 – 1%).[38] Frequency sweeps were conducted from 0.01 to 100 rad/s with a constant shear strain of 1%, all within the linear viscoelastic region.

Statistical Data Analysis. Rheology datasets were analyzed using a two-sided, independent sample t-test to compare the experimental shear elastic modulus (G′) of the hydrogel samples with varying biotin concentration. The sample size (*N*) for all experiments and p-values for all statistical analysis were reported in Table S2. All experimental values were written as the mean ± standard deviation in Table S2 and throughout the manuscript unless otherwise noted. All analysis was conducted using Microsoft Excel and GraphPad Prism 9. For post-processing, any data that were over 2 standard deviations of the mean were considered as outliers and were removed.

Theoretical Network Model Calculations. According to methods in the referenced articles[35, 38, 45], theoretical shear G′ was calculated using affine and phantom polymer network models (Table S3).

Bioerosion Test. 20 μL of hydrogels with either 0 or 10 mM biotin were centrifuged in 1.5 mL microcentrifuge tubes to ensure that all the sample reaches to the bottom. Then, 180 μL of 20 mM

Tris buffer (pH 8.0) with or without 10 mM biotin were gently pipetted in each microcentrifuge tube. All samples were incubated at 37 °C without any mechanical agitation. To reduce evaporation of the buffer, each tube was wrapped with parafilm. At each time point, the absorbance of 1 μL of the centrifuged supernatant was measured using a Nanophotometer P-330 and a submicroliter cell with a pathlength of 1 mm (Implen, Westlake Village, CA, USA). The sample size of each time point was in triplicate ($N = 3$), with three separate hydrogel samples measured.

ASSOCIATED CONTENT

Supporting Information

Supporting Information is available free of charge from ACS Applied Materials & Interfaces or from the corresponding author.

Additional AFM-based SMFS, rheological characterization, and bioerosion results; amino acid sequences; LC/MS and theoretical molecular weight; predictions of theoretical shear elastic moduli based on network models. (PDF)

AUTHOR INFORMATION

Corresponding Author

Minkyu Kim - *Department of Biomedical Engineering, University of Arizona, Tucson, AZ, 85721, USA; Department of Mechanical Engineering and Materials Science, Duke University, Durham, NC, 27708, USA; Department of Materials Science and Engineering, University of Arizona, Tucson, AZ, 85721, USA; BIO5 Institute, University of Arizona, Tucson, AZ, 85719, USA;* minkyukim@arizona.edu

Authors

Samuel Kim - *Department of Biomedical Engineering, University of Arizona, Tucson, AZ, 85721, USA*

Marcus V. J. Cathey - *Department of Biomedical Engineering, University of Arizona, Tucson, AZ, 85721, USA*

Brandon C. Bounds - *Department of Biomedical Engineering, University of Arizona, Tucson, AZ, 85721, USA*

Zackary Scholl - *Department of Mechanical Engineering and Materials Science, Duke University, Durham, NC, 27708, USA*

Piotr E. Marszalek - *Department of Mechanical Engineering and Materials Science, Duke University, Durham, NC, 27708, USA*

Author Contributions

M.K. initiated the project; S.K., P.E.M, and M.K. designed all experiments; S.K., M.V.J.C., B.C.B., and M.K. performed experiments; S.K., Z.S., P.E.M, and M.K. performed data analysis; S.K. and M.K. wrote the original draft; S.K., Z.S., P.E.M, and M.K. edited the manuscript.

Notes

S.K. and M.K. are inventors of a pending US patent application (#18/365,648) assigned to the University of Arizona. This patent pertains to the use of (strept)avidin for constructing polymer networks and hydrogels, as well as the use of biotin and its derivatives to control their mechanical properties. Otherwise, the authors declare no competing financial interests.

ACKNOWLEDGMENT

This work was supported by Tech Launch Arizona Asset Development Program at the University of Arizona and the National Science Foundation (NSF) CAREER Grant (DMR-

2143126). M.V.J.C. was partially supported by the W.L. Gore Scholar Program. PM is currently supported by NSF MCB 1817556 and 2118357 grants.

REFERENCES

(1) Pieters, B. J.; van Eldijk, M. B.; Nolte, R. J.; Mecinovic, J. Natural Supramolecular Protein Assemblies. *Chem Soc Rev* **2016**, *45* (1), 24-39, 10.1039/C5CS00157A.
(2) Sun, H.; Luo, Q.; Hou, C.; Liu, J. Nanostructures Based on Protein Self-Assembly: From Hierarchical Construction to Bioinspired Materials. *Nano Today* **2017**, *14*, 16-41.
(3) Langton, M. J. Engineering of Stimuli-Responsive Lipid-Bilayer Membranes Using Supramolecular Systems. *Nat Rev Chem* **2021**, *5* (1), 46-61.
(4) Jones, S.; Thornton, J. M. Principles of Protein-Protein Interactions. *Proc Natl Acad Sci U S A* **1996**, *93* (1), 13-20.
(5) Li, Y.; Xue, B.; Cao, Y. 100th Anniversary of Macromolecular Science Viewpoint: Synthetic Protein Hydrogels. *ACS Macro Lett* **2020**, *9* (4), 512-524.
(6) Webber, M. J.; Appel, E. A.; Meijer, E. W.; Langer, R. Supramolecular Biomaterials. *Nat Mater* **2016**, *15* (1), 13-26.
(7) Wang, H.; Heilshorn, S. C. Adaptable Hydrogel Networks with Reversible Linkages for Tissue Engineering. *Adv Mater* **2015**, *27* (25), 3717-3736.
(8) Hussey, G. S.; Dziki, J. L.; Badylak, S. F. Extracellular Matrix-Based Materials for Regenerative Medicine. *Nature Reviews Materials* **2018**, *3* (7), 159-173.
(9) Shen, W.; Zhang, K.; Kornfield, J. A.; Tirrell, D. A. Tuning the Erosion Rate of Artificial Protein Hydrogels through Control of Network Topology. *Nat Mater* **2006**, *5* (2), 153-158.
(10) Hu, X.; Li, H. Force Spectroscopy Studies on Protein-Ligand Interactions: A Single Protein Mechanics Perspective. *FEBS Lett* **2014**, *588* (19), 3613-3620.
(11) Scholl, Z. N.; Yang, W.; Marszalek, P. E. Direct Observation of Multimer Stabilization in the Mechanical Unfolding Pathway of a Protein Undergoing Oligomerization. *Acs Nano* **2015**, *9* (2), 1189-1197.
(12) Junker, J. P.; Ziegler, F.; Rief, M. Ligand-Dependent Equilibrium Fluctuations of Single Calmodulin Molecules. *Science* **2009**, *323* (5914), 633-637.
(13) Wang, C. C.; Tsong, T. Y.; Hsu, Y. H.; Marszalek, P. E. Inhibitor Binding Increases the Mechanical Stability of Staphylococcal Nuclease. *Biophys J* **2011**, *100* (4), 1094-1099.
(14) Liang, J.; Fernandez, J. M. Mechanochemistry: One Bond at a Time. *Acs Nano* **2009**, *3* (7), 1628-1645.
(15) Puchner, E. M.; Gaub, H. E. Force and Function: Probing Proteins with Afm-Based Force Spectroscopy. *Curr Opin Struct Biol* **2009**, *19* (5), 605-614.
(16) Hendrickson, W. A.; Pahler, A.; Smith, J. L.; Satow, Y.; Merritt, E. A.; Phizackerley, R. P. Crystal Structure of Core Streptavidin Determined from Multiwavelength Anomalous Diffraction of Synchrotron Radiation. *Proc Natl Acad Sci U S A* **1989**, *86* (7), 2190-2194.
(17) Weber, P. C.; Ohlendorf, D. H.; Wendoloski, J. J.; Salemme, F. R. Structural Origins of High-Affinity Biotin Binding to Streptavidin. *Science* **1989**, *243* (4887), 85-88.
(18) Green, N. M. Avidin. *Adv Protein Chem* **1975**, *29*, 85-133.

(19) Florin, E. L.; Moy, V. T.; Gaub, H. E. Adhesion Forces between Individual Ligand-Receptor Pairs. *Science* **1994**, *264* (5157), 415-417.
(20) Moy, V. T.; Florin, E. L.; Gaub, H. E. Intermolecular Forces and Energies between Ligands and Receptors. *Science* **1994**, *266* (5183), 257-259.
(21) Wong, S. S.; Joselevich, E.; Woolley, A. T.; Cheung, C. L.; Lieber, C. M. Covalently Functionalized Nanotubes as Nanometre-Sized Probes in Chemistry and Biology. *Nature* **1998**, *394* (6688), 52-55.
(22) Merkel, R.; Nassoy, P.; Leung, A.; Ritchie, K.; Evans, E. Energy Landscapes of Receptor-Ligand Bonds Explored with Dynamic Force Spectroscopy. *Nature* **1999**, *397* (6714), 50-53.
(23) Hinterdorfer, P.; Ebner, A.; Gruber, H.; Kapon, R.; Reich, Z. Molecular Recognition Force Microscopy: From Molecular Bonds to Complex Energy Landscapes. In *Handbook of Nanotechnology*, 3rd ed.; Bhushan, B., Ed.; Springer, 2010; pp 763-785.
(24) Freitag, S.; Le Trong, I.; Klumb, L. A.; Chu, V.; Chilkoti, A.; Stayton, P. S.; Stenkamp, R. E. X-Ray Crystallographic Studies of Streptavidin Mutants Binding to Biotin. *Biomol Eng* **1999**, *16* (1-4), 13-19.
(25) Sano, T.; Cantor, C. R. Intersubunit Contacts Made by Tryptophan-120 with Biotin Are Essential for Both Strong Biotin Binding and Biotin-Induced Tighter Subunit Association of Streptavidin. *Proc Natl Acad Sci USA* **1995**, *92* (8), 3180-3184.
(26) Wu, S. C.; Wong, S. L. Engineering Soluble Monomeric Streptavidin with Reversible Biotin Binding Capability. *J Biol Chem* **2005**, *280* (24), 23225-23231.
(27) Gonzalez, M.; Argarana, C. E.; Fidelio, G. D. Extremely High Thermal Stability of Streptavidin and Avidin Upon Biotin Binding. *Biomol Eng* **1999**, *16* (1-4), 67-72.
(28) Kim, M.; Wang, C. C.; Benedetti, F.; Rabbi, M.; Bennett, V.; Marszalek, P. E. Nanomechanics of Streptavidin Hubs for Molecular Materials. *Adv Mater* **2011**, *23* (47), 5684-5688.
(29) Li, Y.; Champion, J. A. Photocrosslinked, Tunable Protein Vesicles for Drug Delivery Applications. *Adv Healthc Mater* **2021**, *10* (15), e2001810.
(30) Erol, O.; Pantula, A.; Liu, W.; Gracias, D. H. Transformer Hydrogels: A Review. *Advanced Materials Technologies* **2019**, *4* (4), 1900043.
(31) Kim, M.; Wang, C. C.; Benedetti, F.; Marszalek, P. E. A Nanoscale Force Probe for Gauging Intermolecular Interactions. *Angew Chem Int Ed Engl* **2012**, *51* (8), 1903-1906.
(32) Carrion-Vazquez, M.; Oberhauser, A. F.; Fowler, S. B.; Marszalek, P. E.; Broedel, S. E.; Clarke, J.; Fernandez, J. M. Mechanical and Chemical Unfolding of a Single Protein: A Comparison. *Proc Natl Acad Sci U S A* **1999**, *96* (7), 3694-3699.
(33) Popa, I.; Berkovich, R.; Alegre-Cebollada, J.; Badilla, C. L.; Rivas-Pardo, J. A.; Taniguchi, Y.; Kawakami, M.; Fernandez, J. M. Nanomechanics of Halotag Tethers. *Journal of the American Chemical Society* **2013**, *135* (34), 12762-12771.
(34) Chilkoti, A.; Tan, P. H.; Stayton, P. S. Site-Directed Mutagenesis Studies of the High-Affinity Streptavidin-Biotin Complex: Contributions of Tryptophan Residues 79, 108, and 120. *Proc Natl Acad Sci U S A* **1995**, *92* (5), 1754-1758.
(35) Knoff, D. S.; Kim, S.; Fajardo Cortes, K. A.; Rivera, J.; Cathey, M. V. J.; Altamirano, D.; Camp, C.; Kim, M. Non-Covalently Associated Streptavidin Multi-Arm Nanohubs Exhibit Mechanical and Thermal Stability in Cross-Linked Protein-Network Materials. *Biomacromolecules* **2022**, *23* (10), 4130-4140.
(36) Wang, X. W.; Zhang, W. B. Spytag-Spycatcher Chemistry for Protein Bioconjugation in Vitro and Protein Topology Engineering in Vivo. *Methods Mol Biol* **2019**, *2033*, 287-300.

(37) Zakeri, B.; Fierer, J. O.; Celik, E.; Chittock, E. C.; Schwarz-Linek, U.; Moy, V. T.; Howarth, M. Peptide Tag Forming a Rapid Covalent Bond to a Protein, through Engineering a Bacterial Adhesin. *Proc Natl Acad Sci U S A* **2012**, *109* (12), E690-697.
(38) Knoff, D. S.; Szczublewski, H.; Altamirano, D.; Cortes, K. A. F.; Kim, M. Cytoskeleton-Inspired Artificial Protein Design to Enhance Polymer Network Elasticity. *Macromolecules* **2020**, *53* (9), 3464-3471.
(39) Lee, G.; Abdi, K.; Jiang, Y.; Michaely, P.; Bennett, V.; Marszalek, P. E. Nanospring Behaviour of Ankyrin Repeats. *Nature* **2006**, *440* (7081), 246-249.
(40) Chen, H.; Zhang, J.; Yu, W.; Cao, Y.; Cao, Z.; Tan, Y. Control Viscoelasticity of Polymer Networks with Crosslinks of Superposed Fast and Slow Dynamics. *Angewandte Chemie International Edition* **2021**, *60* (41), 22332-22338.
(41) Grindy, S. C.; Learsch, R.; Mozhdehi, D.; Cheng, J.; Barrett, D. G.; Guan, Z.; Messersmith, P. B.; Holten-Andersen, N. Control of Hierarchical Polymer Mechanics with Bioinspired Metal-Coordination Dynamics. *Nature Materials* **2015**, *14* (12), 1210-1216.
(42) Yount, W. C.; Loveless, D. M.; Craig, S. L. Strong Means Slow: Dynamic Contributions to the Bulk Mechanical Properties of Supramolecular Networks. *Angewandte Chemie International Edition* **2005**, *44* (18), 2746-2748.
(43) Huang, Z.; Yang, L.; Liu, Y.; Wang, Z.; Scherman, O. A.; Zhang, X. Supramolecular Polymerization Promoted and Controlled through Self-Sorting. *Angewandte Chemie International Edition* **2014**, *53* (21), 5351-5355.
(44) Gu, Y.; Zhao, J.; Johnson, J. A. A (Macro)Molecular-Level Understanding of Polymer Network Topology. *Trends in Chemistry* **2019**, *1* (3), 318-334.
(45) Zhong, M.; Wang, R.; Kawamoto, K.; Olsen, B. D.; Johnson, J. A. Quantifying the Impact of Molecular Defects on Polymer Network Elasticity. *Science* **2016**, *353* (6305), 1264-1268.
(46) Safranski, D. L.; Weiss, D.; Clark, J. B.; Taylor, W. R.; Gall, K. Semi-Degradable Poly(Beta-Amino Ester) Networks with Temporally Controlled Enhancement of Mechanical Properties. *Acta Biomater* **2014**, *10* (8), 3475-3483.
(47) Sun, F.; Zhang, W.-B.; Mahdavi, A.; Arnold, F. H.; Tirrell, D. A. Synthesis of Bioactive Protein Hydrogels by Genetically Encoded Spytag-Spycatcher Chemistry. *Proceedings of the National Academy of Sciences* **2014**, *111* (31), 11269-11274.
(48) Olsen, B. D.; Kornfield, J. A.; Tirrell, D. A. Yielding Behavior in Injectable Hydrogels from Telechelic Proteins. *Macromolecules* **2010**, *43* (21), 9094-9099.
(49) Lou, J.; Mooney, D. J. Chemical Strategies to Engineer Hydrogels for Cell Culture. *Nat Rev Chem* **2022**, *6* (10), 726-744.
(50) Oberhauser, A. F.; Marszalek, P. E.; Erickson, H. P.; Fernandez, J. M. The Molecular Elasticity of the Extracellular Matrix Protein Tenascin. *Nature* **1998**, *393* (6681), 181-185.
(51) Selvin, P. R.; Ha, T. *Single-Molecule Techniques : A Laboratory Manual*; Cold Spring Harbor Laboratory Press, 2008.
(52) Florin, E. L.; Rief, M.; Lehmann, H.; Ludwig, M.; Dornmair, C.; Moy, V. T.; Gaub, H. E. Sensing Specific Molecular Interactions with the Atomic Force Microscope. *Biosensors and Bioelectronics* **1995**, *10* (9-10), 895-901.
(53) Scholl, Z. N.; Marszalek, P. E. Afm-Based Single-Molecule Force Spectroscopy of Proteins. *Methods Mol Biol* **2018**, *1814*, 35-47.
(54) Sano, T.; Cantor, C. R. [19] Streptavidin-Containing Chimeric Proteins: Design and Production. In *Methods in Enzymology*, Vol. 326; Academic Press, 2000; pp 305-311.

Table of Contents